Journal of Hazardous Materials 172 (2009) 187–195

Contents lists available at ScienceDirect

Journal of Hazardous Materials

journal homepage: www.elsevier.com/locate/jhazmat

Study of the electrochemical oxidation and reduction of C.I. Reactive Orange 4 in sodium sulphate alkaline solutions

A.I. del Río, J. Molina, J. Bonastre, F. Cases*

Departamento de Ingeniería Textil y Papelera, Escuela Politécnica Superior de Alcoy, Universidad Politécnica de Valencia. Plaza Ferrándiz y Carbonell, s/n, 03801, Alcoy, Alicante, Spain

ARTICLE INFO

Article history:
Received 9 April 2009
Received in revised form 22 June 2009
Accepted 28 June 2009
Available online 4 July 2009

Keywords:
Electrochemical reduction
Stainless steel
Reactive dye
Organic coating
Decolourisation
Anodic oxidation

ABSTRACT

Synthetic solutions of hydrolysed C.I. Reactive Orange 4, a monoazo textile dye commercially named Procion Orange MX-2R (PMX2R) and colour index number C.I. 18260, was exposed to electrochemical treatment under galvanostatic conditions and Na_2SO_4 as electrolyte. The influence of the electrochemical process as well as the applied current density was evaluated. Ti/SnO_2–Sb–Pt and stainless steel electrodes were used as anode and cathode, respectively, and the intermediates generated on the cathode during electrochemical reduction were investigated. Aliquots of the solutions treated were analysed by UV–visible and FTIR-ATR spectroscopy confirming the presence of aromatic structures in solution when an electro-reduction was carried out. Electro-oxidation degraded both the azo group and aromatic structures. HPLC measures revealed that all processes followed pseudo-first order kinetics and decolourisation rates showed a considerable dependency on the applied current density. CV experiments and XPS analyses were carried out to study the behaviour of both PMX2R and intermediates and to analyse the state of the cathode after the electrochemical reduction, respectively. It was observed the presence of a main intermediate in solution after an electrochemical reduction whose chemical structure is similar to 2-amino-1,5-naphthalenedisulphonic acid. Moreover, the analysis of the cathode surface after electrochemical reduction reveals the presence of a coating layer with organic nature.

1. Introduction

It is generally well accepted that colour in waterways is an aesthetic problem rather than an ecotoxic hazard. The Ecological and Toxicological Association of Dyes and Organic Pigment Manufacturers (ETAD) has, over the last 30 years, been pioneering in promoting an understanding of the human health and environment impacts of colourants and contributing to the body of knowledge in these areas. Thus, the impact and toxicity of dyes in the environment have been extensively studied [1,2]. However, the knowledge concerning their carcinogenic, mutagenic and bactericide properties is still incomplete since there is a large variety of dyes. Different treatments to decolourise and degrade dyeing wastewaters have then attracted increasing interest since the large majority of these dyes are not degradable in conventional wastewaters treatment plants [3]. A wide range of methods have been developed for this purpose. Ozonation [4], advanced oxidation processes [5–8], enzymatic [9] or adsorption processes [10] have been studied recently for the removal of different dyes. Over the past 10 years, the electrochemical techniques have been found of special interest for wastewater remediation [11–14]. Among all their advantages, it is interesting to notice the high yields of removal/degradation of polluting substances with maximum energy resource management. These techniques show facility and precision on control of the electrochemical process (since the electron is the main reagent) and a compact design [15]. To improve the electrochemical treatment efficiency, many researches have been focused on the electrode development. Various types of electrodes such as graphite [16], activated carbon fibre [17], Pt [18–21] and boron doped diamond electrodes (BDD) [22–25] have been studied but, in the last years, Dimensionally Stable Anodes (DSA) have arisen great interest as one of the promising electrodes. Currently, their use for the degradation of organic pollutants is an active area of research [26–29]. In this sense, anodes coated with SnO_2 exhibit high overpotential for oxygen (η_{O_2}) and chlorine evolution [30,31], good stability, low resistivity and high electrical conductivity (thanks to doping). They are known as "non-active" electrodes because they do not participate in the oxidation; they only provide adsorption sites for the radicals $^{\bullet}OH_{ads}$ generated as a result of water discharge (Eq. (1)).

$$H_2O \rightarrow {}^{\bullet}OH_{ads} + H^+ + e^- \quad (1)$$

On the other hand, as far as it is known, the efficiency of the electrochemical oxidation is also in direct relation to supporting medium. Then, an extensive range of electrolytes have been

* Corresponding author. Tel.: +34 96 652 84 12/11; fax: +34 96 652 84 38.
E-mail address: fjcases@txp.upv.es (F. Cases).

0304-3894/$ – see front matter © 2009 Elsevier B.V. All rights reserved.
doi:10.1016/j.jhazmat.2009.06.147

employed such as H_2SO_4 [32,33], KNO_3 [34], $HClO_4$ [27], NaF [32], Na_2SO_4 [17,35–41] and NaCl (or KCl) [35–37,41–49]. From all these supporting electrolytes, the role of chloride is important since the colour removal and degradation degree of azo dyes obtained may be enhanced. However, although DSA-type electrodes are usually preferred due to their high stability, the large production of oxidant ClO^- in a chlorinated medium affects directly to the electrode material stability. This fact reduces its service life and gives undesirable toxic chlorinated by-products. In this sense, sulphate is an inert supporting electrolyte which does not produce any reactive species during the electrolysis, except under special conditions where it may generate persulphate [50–53].

Recently, electrochemical reduction has been found as an interesting method for a suitable decolourisation of wastewaters containing dyes. Nevertheless, the number of papers that have been published dealing with the direct electro-reduction of dyes is limited and studies of surface modification of the cathode during the electrolysis and its influence in the electrode activity is not reported. The electro-reduction process of Amaranth solutions was investigated by Fan et al. [17,53]. Working under galvanostatic conditions it was obtained a 95% of colour removal. On the other hand, it has been demonstrated that the cathodic reduction of dyes containing azo groups was possible by the use of iron-TEA as mediator system and a stainless steel multi-cathode cell electrically connected with one or two anodes. This configuration allows the operation of the cell with a maximum cathode area and minimum anode area [54,55].

Reactive dyes are one of the most significant technological innovations of the 20th century in the dyes field. However, the fixation reaction of these dyes is hindered by another competitive reaction consisting on the dye hydrolysis. This is the reason why reactive dyes are only retained from 60 to 90% at best case on cellulose fibres. For this reason they are one of the major responsible of coloured rivers. An additional problem is that reactive dyes in both its ordinary and hydrolysed forms are not easily biodegradable and thus even after extensive treatment, colour from unexhausted reactive dyes may still remain in textile wastewater.

In this work, we will evaluate the electrochemical oxidation and reduction of an azo/dichlorotriazine reactive dye: C.I. Reactive Orange 4 (commercially named Procion Orange MX-2R, PMX2R, and Colour Index Number 18260), in the presence of Na_2SO_4 as electrolyte. Doped SnO_2 and stainless steel electrodes were employed as anode and cathode, respectively and the evaluation of intermediates interferences is carried out in order to explain the supposed loss of electroactivity of the cathode during the treatment. This dye was selected as a representative dye with a 1,3,5-triazinyl group as a functional group. Procion MX dyes present a hydrolysed unfixed form that can amount to as much as 15–40% of the total applied [56].

2. Materials and methods

2.1. Chemicals

Ultrapure water from an Elix 3 Millipore Milli-Q RG system with a resistivity near to 18.2 MΩ cm was used for the preparation of all solutions. Dye solutions were simulated from the commercial product (supplied by Zeneca) according to real concentrations found in textile effluents.

Taking into account that the hydrolysed form of the dye is responsible for colour in effluents containing wastewaters from textile industry, all synthetic dye solutions were hydrolysed previously by NaOH solution addition. As a result of this process, all dye solutions presented an alkaline pH (about 10–13) where two chlorine atoms of the dye molecule were replaced by two OH groups.

Blank solutions with the corresponding supporting electrolytes were also prepared and used in a separate compartment. These solutions consisted of 0.5 M NaOH (Merck p.a.) + 0.1/0.5 M Na_2SO_4 (Merck p.a.). It is important to highlight that NaOH was only used to obtain the same alkaline pH as the dye solutions, and Na_2SO_4 was the electrolyte.

2.2. Electrolyses

The electrolyses of the alkaline aqueous solutions of hydrolysed dye were carried out in divided electrolytic cells. This allowed us to study separate processes of electro-reduction and electro-oxidation. The convenient separation between anode and cathode compartments was achieved with a Nafion 117 (Du Pont) cationic membrane. The dye molecule has an anionic nature in solution; for this reason, an anionic membrane could not be used since the huge molecular weight of the dye and the applied current density made the membrane blocked. A cylindrical stainless steel electrode was employed as cathode in all cases. The chemical composition and diameter are the same as those for the working electrode of voltammetric experiments. The anodes were: a platinum wire when electro-reduction process was studied and a Ti/SnO_2–Pt–Sb electrode when electro-oxidation was carried out. The volume of solution to be treated was 55 mL in every case and the area of the electrodes was 2 cm^2. The homogeneous nature of the medium during the electrolyses was maintained using magnetic stirring. The dye concentration selected for electrolytic experiments was 0.8 g L^{-1}. This value is included in the range of real dye concentration found in textile effluents [57]. All the experiments were carried out under galvanostatic conditions with a power supply (Model Grelco GVD310 0–30 Vcc/0–10 A). The applied current densities were 125 and 250 mA cm^{-2} until a total loaded charge of 227 Ah L^{-1}. Then, the final samples could be compared at constant experimental conditions.

2.3. Preparation of the electrodes

With the purpose of obtaining the maximum reproducibility in voltammetric experiments and electrolyses, both the platinum and the stainless steel electrode underwent a pre-treatment. The platinum electrode required a flame thermic treatment before each electrochemical experiment according to the method developed by Clavilier [58].

The stainless steel electrode required a pre-treatment consisting of a mechanical polishing of the electrode and immediately afterwards a cleaning with acetone was carried out. Finally, a polishing of the working electrode with 1.0, 0.3 and 0.05 μm alumina slurry was performed cleaning the electrode with ultrapure water after every polishing session. At this point, a cathodic treatment was made on the electrode surface in order to eliminate the oxide traces.

The electrodes of doped tin dioxide used in electrochemical experiments for oxidation processes were prepared following a standard thermal decomposition method of the salt precursor on a titanium substrate [59–62]. Titanium plates (1 cm × 1 cm) were first pre-treated in order to eliminate the superficial layer of TiO_2 (an electric semiconductor) and to obtain a higher roughness. Thus, the electrocatalytic oxide deposit could adhere to the support. This pre-treatment consisted of degreasing with acetone using ultrasounds for 10 min. Following, the titanium supports were etched for 1 h in a boiling solution of oxalic acid (10%). After that, the supports were rinsed with ultrapure water and the precursor solution was brushed on the Ti plate. This precursor solution contained 10% $SnCl_4{\cdot}5H_2O$ (provided by Aldrich) + 1% $SbCl_3$ (purchased from Fluka) + 0.252% $H_2PtCl_6{\cdot}6H_2O$ (supplied by Merck) dissolved in a mixture of ethanol (provided by Panreac) + HCl (supplied by Merck). Afterwards, the electrodes were introduced in an oven at 400 °C for

10 min. In this phase of the procedure, the decomposition of the salt and the formation of the metal oxide take place. This process was repeated until a weight increment of about 2 mg cm^{-2}. Finally, a final thermal treatment at 600 °C was applied for 1 h.

2.4. Analyses and instruments

2.4.1. Cyclic voltammetry

All voltammetric measurements were performed using an Eco-Chemie Autolab PGSTAT30 potentiostat/galvanostat at room temperature. Oxygen was previously removed from all solutions by bubbling nitrogen for 30 min to remove oxygen prior to the experimental runs and the solution was protected under nitrogen atmosphere during the experiments. A three electrode electrochemical cell was used. The system consisted of a cylindrical stainless steel working electrode (chemical composition in wt.%: C ≤ 0.050, Si 0.750, Mn ≤ 2.000, P 0.040, S 0.015, Cr 18–19, Cu 8.5–9) with 4 mm diameter and a Ag/AgCl (KCl 3 M) reference electrode. A platinum wire was used as counter electrode. Voltammetric measurements revealed similar results when both 0.1 and 0.5 M Na_2SO_4 were used as background electrolyte so only those results obtained with 0.1 M Na_2SO_4 will be shown. Voltammetric studies were performed at different dye concentrations: 0.08, 0.8 and 3.9 g L^{-1} since textile effluents concentrations vary from 0.01 to 0.25 g L^{-1} reaching concentrations about 1 g L^{-1} in some cases [57].

2.4.2. Spectroscopical techniques

The UV–visible spectra of PMX2R and its evolution during the electrolysis were recorded using a Genesys 10 UV Scanning spectrophotometer. Fourier Transform Infrared Attenuated Total Reflection (FTIR-ATR) experiments were performed with a Nicolet Magna 550 Spectrometer equipped with DTGS detector in order to monitor the functional groups evolution during the electrolysis. X-ray photoelectron spectroscopy (XPS) analyses were performed at a base pressure of at 5×10^{-10} mbar and a temperature around 173 K. The XPS spectra were obtained with a VG-Microtech Multilab electron spectrometer using unmonochromatized Mg Kα (1253.6 eV) radiation form a twin anode source operating at 300 W (20 mA, 15 kV). The binding energy (BE) scale was calibrated with reference to the C 1s line at 284.6 eV.

2.4.3. Chromatographic techniques

High Performance Liquid Chromatography (HPLC) analysis was performed using a Hitachi Elite Lachrom Chromatographic System equipped with diode array detector. The chromatographic separations were performed on a Lichrospher 100 RP-18C column with 5 μm packing. Mobile phase composition was methanol (eluent A)/aqueous buffer solution KH_2PO_4·Na_2HPO_4 (eluent B) with pH 6.9. Separation was accomplished at a flow rate of 1 mL min^{-1}, at 25 °C and injection volume of 80 μL. The detection wavelength was set at 486 and 250 nm. At the beginning of the chromatographic separations, the gradient elution consisted of 15% methanol–85% aqueous buffer and it was progressively modified to 30% methanol–70% aqueous buffer during 10 min.

In order to identify the major intermediates formed along the process, Gas Chromatography–Mass Spectrometry (GC–MS) analyses were carried out. A Shimadzu GCMS-QP2010 gas chromatograph–mass spectrometer equipped with a secondary electron multiplicator dinode (MSD) was used. The capillary column was a Teknokroma S Meta X5, P/N TR-820232 (30 m × 0.25 mm I.D. and 0.25 μm film thickness). The analyses were carried out by a splitless injection mode (1 μL) with a helium carrier flow of 30 mL min^{-1} and inlet set at 250 °C. The oven temperature program was first set at 140 °C for 4 min and then brought to 275 °C at a rate of 10 °C min^{-1}. The mass spectrometry analyser operated in the electron impact mode with a scan of m/z 40–1000, scan speed of 2000, at 0.5 s intervals and ion source temperature of 200 °C.

3. Results and discussion

3.1. Electrolysis assays

3.1.1. UV–visible spectroscopy

Typical UV–visible spectra for untreated and treated dye solutions have been done and changes in absorbance of dye solutions were investigated, as shown in Fig. 1. A divided electrolytic cell was used for the electrolytic treatments. It is important to highlight the assumption of the degradation reaction as the predominant process. The initial spectra showed that the wavelength of maximum absorbance (λ_{max}) was 486 nm in the visible region and corresponds to the azo group. In addition, the aromatic rings absorbance was observed between 200 and 300 nm, in the UV region. In order to perceive distinctions between intermediates and initial dye structures, both the azo group and the aromatic rings absorbance were monitored during the electrolytic processes. Fig. 1 shows the UV–visible spectra of the initial solution (I) and final solution after the electro-reduction (II) and electro-oxidation (III) assays at 125 mA cm^{-2} and in presence of 0.1 M Na_2SO_4 as electrolyte (227 Ah L^{-1}). The azo group was completely destroyed after an electro-reduction process but the aromatic structures remained in solution although in minor quantity. In contrast, the electro-oxidation (III) showed a considerable degradation of the dye structure which is in accordance with the TOC and COD removal percentages observed for this process. At the experimental conditions commented above, it was obtained a 55% and a 75% of TOC and COD removal. These results lead us to think that the intermediate species generated during the process present an oxidation state more positive than the initial one but some of them remain in solution. As explained in Section 2, at 227 Ah L^{-1} of loaded charge the TOC and COD removals are considered invariable and this permits to compare the final samples at the same conditions. This gave an energetic consumption of 2.56 kW L^{-1} [63].

3.1.2. FTIR-ATR spectroscopy

To confirm the differences observed between electro-oxidation and electro-reduction, horizontal FTIR-ATR spectroscopy was also employed. This technique permitted to demonstrate the evolution of functional groups during electrolyses. The spectra were collected at 8 cm^{-1} resolution as a result of an average of 100 scans with a

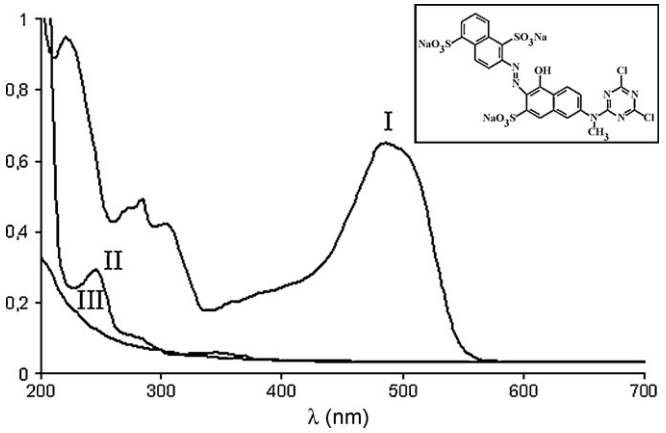

Fig. 1. UV–visible spectra of the initial solution of 0.8 g L^{-1} PMX2R (I) and the final solution after electrochemical reduction (II) and electrochemical oxidation (III). Electrolysis conditions: 0.5 M Na_2SO_4 as electrolyte; current density 125 mA cm^{-2}; total charge loaded 227 Ah L^{-1}; electrode area = 2 cm^2; V_{sol} = 55 mL. Inset figure: chemical structure of PMX2R.

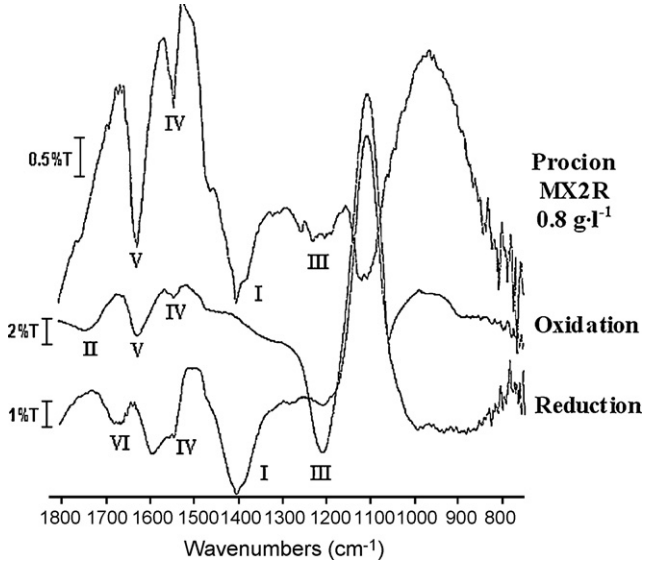

Fig. 2. Comparison of the horizontal FTIR-ATR spectra obtained for the initial dye (concentration 0.8 g L^{-1}) and final solution after an electro-reduction process and an electro-oxidation process at 250 mA cm^{-2} and 0.1 M Na_2SO_4 as electrolyte (loaded charge 227 Ah L^{-1}). Electrolytic cell divided with cationic membrane. Electrode area = 2 cm^2; V_{sol} = 55 mL. Resolution: 8 cm^{-1}. 400 scans. Prism of ZnSe.

ZnSe prism. Fig. 2 shows the spectra of the initial dye solution with a concentration of 0.8 g L^{-1} and those obtained from the samples resulting from electro-oxidation and electro-reduction processes at 227 Ah L^{-1}, respectively. By comparing the differences observed we can conclude the following facts [64]:

i The strong band appeared at 1400 cm^{-1} (I) in the spectrum corresponding to the original dye is related to the aromatic structures –C=C– stretching vibration. Electro-oxidation process eliminated aromatic structures since this band was not observed. On the other hand, the spectrum corresponding to electro-reduction process showed this band indicating the presence of aromatic structures.

ii As a result of the electro-oxidation, a weak band at 1740 cm^{-1} (II) appeared. This can be ascribed to –C=O stretching vibration, maybe related to carbonyls groups. Besides, a band at 1200 cm^{-1} (III) seems to be more intense. This could be because of the partial relation of this band with –C–O bending mode of the carbonyl groups. These bands are not present in the spectrum corresponding to electro-reduction process.

iii The band at 1530 cm^{-1} (IV) can be associated to the –C–N– stretching vibration mode of the triazinic group. Both electro-oxidation and electro-reduction processes degraded this group (at least partially) since this band diminished in both cases.

iv A very sharp strong band at 1620 cm^{-1} (V) was observed in the initial dye spectrum. This transition could indicate the stretching vibration of the imine bond (C=N–) present in the corresponding tautomeric form of the PMX2R molecule. After the electro-reduction process this band split in two weak bands at 1590 and 1670 cm^{-1} which may be attributed to –N–H bending mode as a result of the azo rupture and the formation of the amino group.

3.1.3. Chromatographic analyses

HPLC technique was employed to monitor the diminution in concentration of PMX2R as loaded charge (Ah L^{-1}) increases. Since this technique is specifically useful to study the cleavage of the azo group as well as the formation of intermediates, the decolourisation produced during the electrolyses was studied. Then, representative chromatograms were obtained during electro-oxidation and electro-reduction processes at 125 and 250 mA cm^{-2} with 0.1 M Na_2SO_4 as electrolyte. Fig. 3 shows the UV–visible spectra of the intermediates generated and their corresponding retention times during the electrolyses. All representations shown in Fig. 3 were registered considering that the area of the chromatographic peak of the dye containing the unbroken azo group ($Area_{initial}$) was reduced in 99%. At this point of the electrolysis, the area of the chromatographic peak for the untreated dye corresponds to the presence of only 1% of the intact azo group in solution (that is $Area = 0.01 Area_{initial}$). As was to be expected, the band corresponding to the azo group (centred at 486 nm; visible region) does not appear at this point of the electrolysis in all cases. However, the UV region of these spectra shows substantial differences between

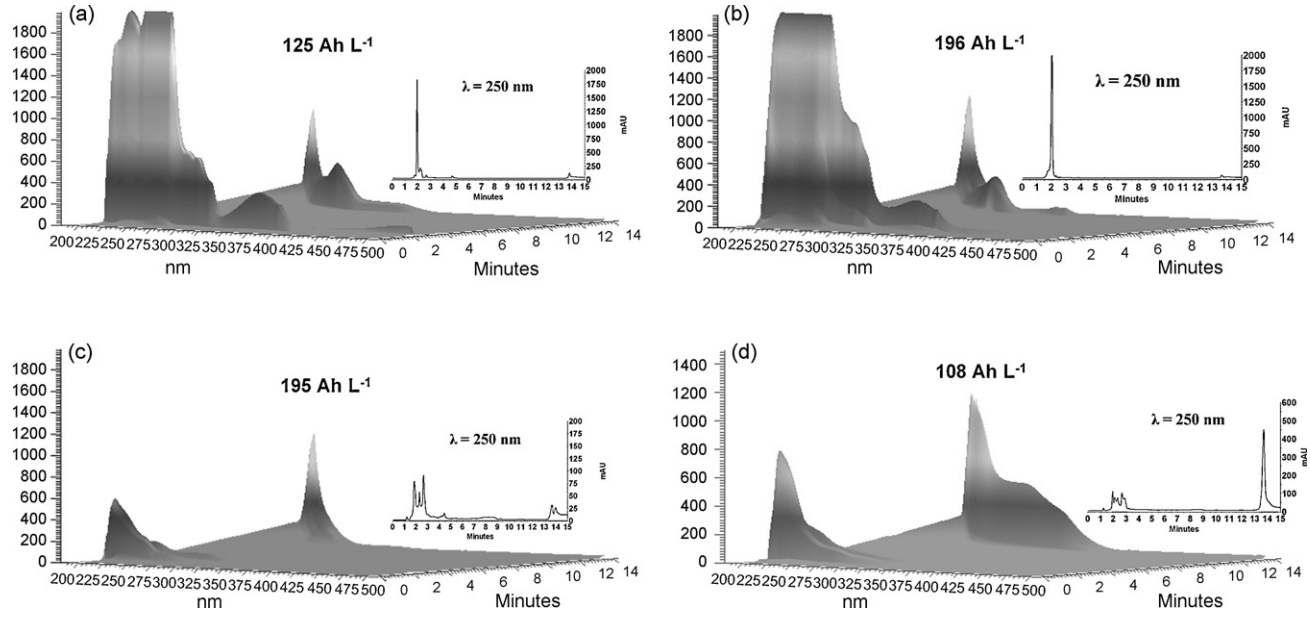

Fig. 3. 3D UV–visible/chromatograms images obtained when $Area = 0.01 Area_{initial}$. (a) Electrochemical reduction at 125 mA cm^{-2}; (b) electrochemical reduction at 250 mA cm^{-2}; (c) electrochemical oxidation at 125 mA cm^{-2}; (d) electrochemical oxidation at 250 mA cm^{-2}. 0.1 M Na_2SO_4 as electrolyte; electrode area = 2 cm^2. Inset figures: chromatograms obtained at 250 nm for each experiment. Loaded charge values (Ah L^{-1}) shown.

electro-reduction and electro-oxidation processes. Thus, at 250 nm (inset figures in Fig. 3a and b), electro-reduction processes shows chromatograms where a main peak is observed for the two current densities employed. It was observed that the area of this chromatographic peak was influenced slightly by the current density applied during the electro-reduction process. However, it is very interesting to highlight that a superficial brown layer appeared onto the stainless steel electrode during the electro-reduction in both cases. Electro-oxidation processes present a different behaviour and, as it can be seen, the height of these bands is one order of magnitude lesser than those obtained in the electro-reduction processes.

As explained above, the spectrum of PMX2R solutions shows the azo group band at about 486 nm. At this wavelength, the chromatogram obtained shows a main peak whose integrated area is in direct relation with the quantity of dye present in solution with this chromophore group intact (figure not shown) [63]. The variation of PMX2R concentration can be evaluated by plotting the evolution of Ln (Area/$Area_{initial}$) versus loaded charge (Ah L^{-1}), as shown in Fig. 4. Then, the decolourisation kinetics and the apparent decolourisation rate constants (k_{app}, s^{-1}) can be determined. In all cases, it was a pseudo-first order kinetic since the chromatographic area varies exponentially with loaded charge (Ah L^{-1}). As shown in Fig. 4, the apparent decolourisation rate constants are influenced by the current density applied. Thus, it was observed that decolourisation obtained by electrochemical oxidation was higher at 250 mA cm^{-2}. In contrast, electrochemical reduction showed the opposite behaviour since increasing current density diminished the decolourisation rate. In fact, when the applied current density was 125 mA cm^{-2}, the loaded charge necessary to reduce in a 99% the quantity of azo group present in solution during the electro-oxidation process was about 195 Ah L^{-1}. At the same conditions, electrochemical reduction processes needed a loaded charge of about 125 Ah L^{-1} (see Fig. 3a and c). When current density was 250 mA cm^{-2}, it was observed that electrochemical oxidation needed 108 Ah L^{-1} to obtain only 1% of the initial quantity of azo group in solution. On the other hand, electrochemical reduction required 196 Ah L^{-1} of loaded charge (see Fig. 3b and d). This is connected with the major generation of sub-products from electrochemical reduction of PMX2R which are responsible for the layer observed on the stainless steel electrode surface. Therefore, the cathode can undergo a greater block of the electrocatalytic activity resulting in a decrease of the decolourisation rate.

Focusing the attention on the electrochemical reduction process carried out at 250 mA cm^{-2}, the intermediates generated during this electrochemical process were studied in order to understand the block of the cathode. Thus, different chromatograms were obtained during the electro-reduction process at 250 mA cm^{-2} and

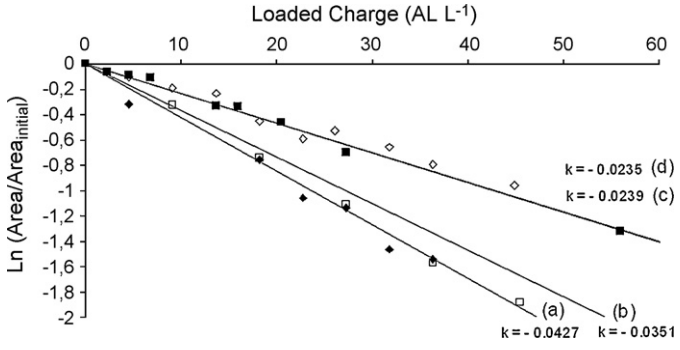

Fig. 4. Logarithm of the normalised chromatographic area of the dye peak versus loaded charge (Ah L^{-1}). (a) Oxidation at 250 mA cm^{-2}; (b) reduction at 125 mA cm^{-2}; (c) oxidation at 125 mA cm^{-2}; (d) reduction at 250 mA cm^{-2}. Synthetic solutions of PMX2R 0.8 g L^{-1} and 0.1 M Na_2SO_4; Electrode area = 2 cm^2; V_{sol} = 55 mL. Chromatographic dye peaks detected at 486 nm.

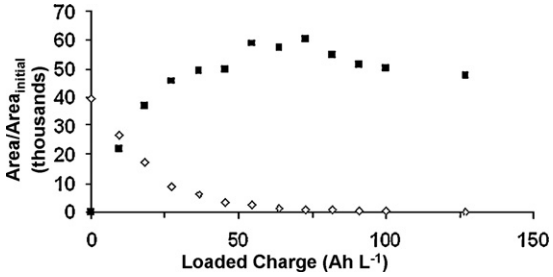

Fig. 5. Evolution of chromatographic areas corresponding to the azo group at 486 nm (◊) and the electro-reduction product at 250 nm (■). Current density: 250 mA cm^{-2}. Synthetic solution of 0.8 g L^{-1} PMX2R with 0.1 M Na_2SO_4 as electrolyte. Electrode area = 2 cm^2; V_{sol} = 55 mL.

0.1 M Na_2SO_4 as electrolyte. The detector wavelength was set at the maximum value of absorbance of the azo group (486 nm). Fig. 5 shows the variation of the dye concentration as a function of the integrated area of the chromatographic peak observed at 486 nm versus loaded charge (Ah L^{-1}). As it can be seen, the azo group was practically removed when the electro-reduction process was performed. On the other hand, when the detector was set at the wavelength absorbance of the aromatic structures (250 nm), it was detected a main chromatographic peak (t_R about 2.0 min) whose area increased with loaded charge (Ah L^{-1}) until a constant value. It can be seen that, as a consequence of the cleavage of the azo group by electrochemical reduction, a stable intermediate was generated in solution. From about 100 Ah L^{-1} on up, the integrated area of this chromatographic peak presents a constant and stabilized value. This behaviour coincides with the complete disappearance of the azo group.

Different commercial compounds with a chemical structure similar to some moieties of the PMX2R molecule were analysed by HPLC (250 nm as detection channel) and UV–visible spectroscopy. From those results, it was observed that 2-amine-1,5-naphthalenedisulphonic acid was the most similar compound to the main electro-reduction intermediate generated during an electrochemical reduction. The reason was the so close values of t_R and a similarity degree of 98.8% obtained by comparing the UV–visible spectra (data not shown). Internal patron assays were also carried out with this commercial product and confirmed this result. According to this, this electro-reduction intermediate should be structurally similar to 2-amine-1,5-naphthalenedisulphonic acid [63].

Preliminary GC–MS analyses carried out in our laboratory corroborated this assumption. Aliquots of a PMX2R solution treated by electrochemical reduction were taken at loaded charge of about 45 Ah L^{-1}, when a complete decolourisation was observed, and at 240 Ah L^{-1} of loaded charge (final sample). Both samples were subjected to a derivatisation process in order to turn sulphonated species (resulting from electrochemical reduction) into more volatile products. For his purpose, the sulphonic groups were chemically reduced to thiol groups using iodide-trifluoroacetic anhydride [65,66]. It was observed that both samples presented the characteristic peaks of derivatized 2-amine-1,5-naphthalenedisulphonic acid (figure not shown). The area of these peaks was higher at 240 Ah L^{-1} so, from these results, it can be deduced that this specie is stable in solution as the information drawn from Fig. 5 revealed.

3.2. Studies of the cathode layer

3.2.1. Cyclic voltammetry

Cyclic voltammetry technique was required for explanation of electrochemical behaviour of both the PMX2R molecule and inter-

mediate species generated during the electrochemical treatment of the dye solution [67,68].

First, a 0.5 M NaOH + 0.5 M Na_2SO_4 medium (blank solution) was chosen to investigate the electrochemical behaviour of the stainless steel electrode in absence of dye. Fig. 6a shows the stabilized voltammogram obtained in these conditions. The curve was obtained at 50 mV s^{-1} and the electrode was first introduced into solution at the open circuit potential value (−1.1 V). After that, the selected potential region was from −1.35 to 0.53 V. The voltammogram was measured using Ag/AgCl, KCl (3 M) reference electrode. As it can be seen, the processes which take place are the oxidation and reduction of the working electrode surface at −0.70 and −1.04 V, respectively. The redox behaviour of chromium contained in the working electrode appeared at 0.48 and 0.36 V for chromium oxidation and oxide reduction, respectively.

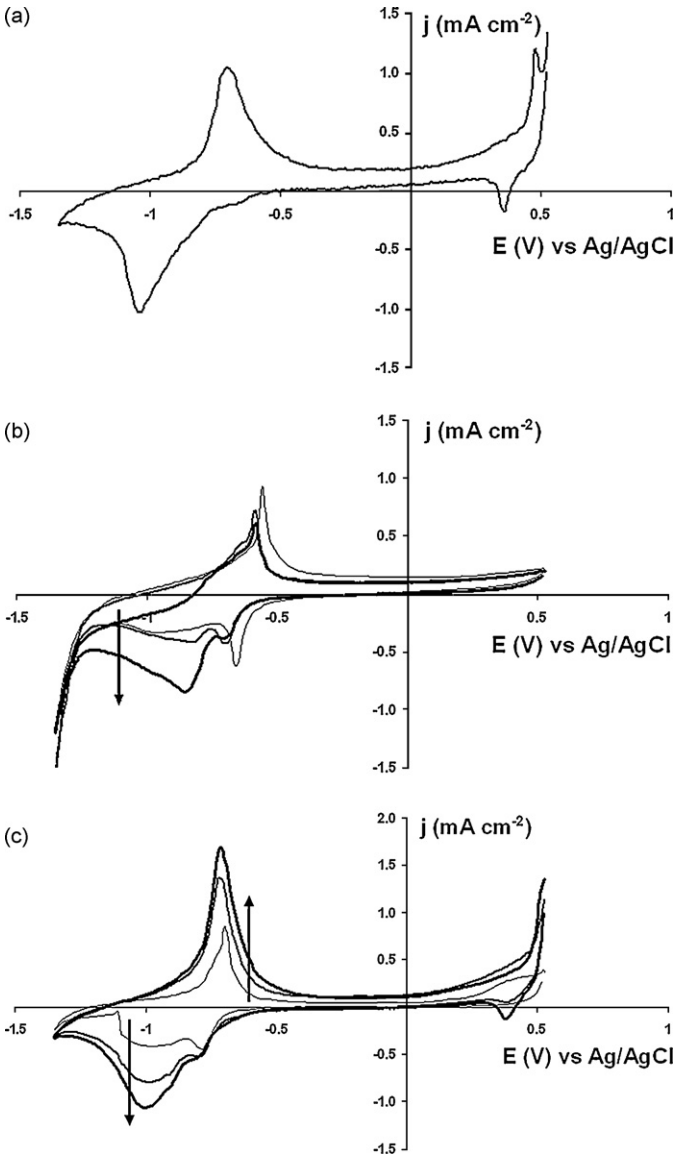

Fig. 6. (a) Cyclic voltammogram of a stainless steel electrode immersed in a blank solution (0.5 M Na_2SO_4 and 0.5 M NaOH). Tenth scan. Scan rate: 50 mV s^{-1}. (b) Effect of increasing the PMX2R concentration on cyclic voltammograms recorded on a stainless steel electrode. Scan rate: 50 mV s^{-1}. Concentrations: 0.08, 0.8 and 3.9 g L^{-1}. Tenth scan. (c) Cyclic voltammograms obtained when the stainless steel electrode was immersed in blank solution after a previous voltammetry assay in a 0.08 g L^{-1} PMX2R solution. Scan rate: 50 mV s^{-1}. First, fifth and tenth scans. All experiments recorded from −1.35 to 0.53 V. Electrode previously introduced into the solution at −1.1 V (open circuit potential).

Fig. 6b shows the stabilized cyclic voltammograms obtained on a stainless steel electrode immersed in PMX2R solution with different concentrations: 0.08, 0.8 and 3.9 g L^{-1}. In presence of PMX2R, a strong oxidation peak was observed at −0.55 V. This peak was related to the dye oxidation. Overlapped to this peak, a small shoulder is presented at −0.61 V corresponding to the surface oxidation. A broad cathodic peak around −0.95 V is appeared in the reverse scans associated to the surface reduction when 0.08 g L^{-1} dye concentration was used. The dye reduction peak, at this dye concentration, was also observed at −0.69 V. It is interesting to notice that, when the dye concentration increases, a new cathodic process is appeared at −0.83 V modifying the corresponding cyclic voltammogram. In fact, this can be clearly observed when a dye solution of 3.9 g L^{-1} concentration was used and it seems to be related to the generation of intermediate species as the concentration increased.

In order to study the adsorption capability of the species present in solution on the stainless steel electrode, a new experience was carried out. After several consecutive cycles of a cyclic voltammetry experiment in PMX2R solution, the electrode was extracted from the electrochemical cell, cleaned carefully with ultrapure water and transferred into a blank solution. After that, a voltammetric experience was carried out at the same conditions. This experiment allows identifying the adsorbed species which could be incorporated to the surface of the electrode. The cyclic voltammograms obtained are shown in Fig. 6c. As it can be seen, a redox response of adsorbed species was observed at −0.69 and −0.77 V for oxidation and a reduction peaks, respectively. The block of the surface as a result of this adsorption was confirmed with the absence of the typical voltammetric peaks of chromium contained in the electrode surface. When a high number of scans were accumulated, the peaks corresponding to the adsorbed species disappeared. Then, the redox behaviour of the stainless steel was only observed as well as the chromium redox behaviour too.

The type of adsorption produced on the stainless steel electrode was studied by performing open circuit assays (figure not shown). The electrode was immersed into a 0.08 g L^{-1} PMX2R solution at open circuit for 15 min. Following, it was gently washed with ultrapure water and introduced into a blank solution where a voltammetric experience was carried out. The cyclic voltammograms registered in this experience would show the influence that the open circuit potential could have on the adsorption produced. It was observed that the voltammograms presented similar shapes to that obtained when a blank solution was studied in the same experimental conditions. This fact confirmed that the adsorption

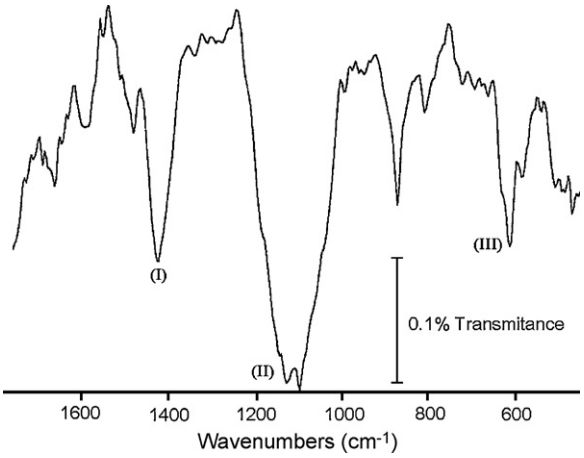

Fig. 7. Vertical FTIR-ATR spectrum of the layer appeared on the stainless steel electrode during the electrochemical reduction of 0.8 g L^{-1} PMX2R and 0.5 M Na_2SO_4 solutions in electrolytic cell divided using a cationic membrane. Electrode area: 4 cm^2. Resolution: 8 cm^{-1}. 400 scans. Prism of KRS5.

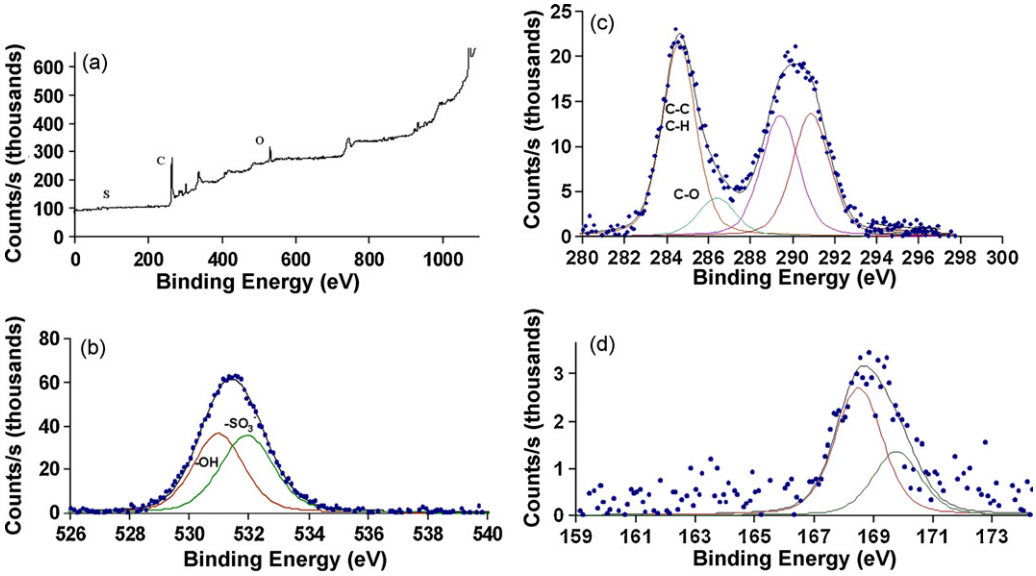

Fig. 8. XPS spectra of the layer appeared during the electrochemical reduction of a 0.8 g L^{-1} PMX2R and 0.5 M Na_2SO_4 solution. Electrode area: 4 cm^2. Electrolytic cell divided using a cationic membrane. (a) XPS general spectrum, (b) oxygen O 1s XPS high resolution spectrum, and (c) carbon C 1s XPS high resolution spectrum. (d) Sulphur S 2p XPS high sensibility spectrum.

observed on the electrode surface (Fig. 6c) occurred as a result of the previous electrochemical treatment.

3.2.2. FTIR-ATR spectroscopy

The layer appeared on the stainless steel electrode during the reduction electrolysis assays was further analysed by vertical FTIR-ATR spectroscopy technique (Fig. 7). The spectrum was collected at 8 cm^{-1} resolution with an average of 400 scan and a KRS5 prism.

The sharp band appeared at 1400 cm^{-1} (I) can be ascribed to the stretching vibration of the C–C bond in the naphthalene structure. Besides, the strong and broad band around 1000–1200 cm^{-1} (II) clearly indicates the –C=C– stretching vibrations of the naphthalene structure. From these results, it can be deduced the presence of naphthalene groups in the layer. Finally, the band of moderate intensity around 590–600 cm^{-1} (III) indicates the presence of iron oxides.

From the FTIR-ATR results it could be deduced the organic nature of the layer taking into account that naphthalene groups are present in the dye structure too.

3.2.3. X-ray photoelectron spectroscopy

The application of surface analytical techniques such as X-ray photoelectron spectroscopy provides molecular information relevant to the electrode surface chemistry. In this sense, a XPS characterisation of the layer was performed. The general XPS spectrum (Fig. 8a) denoted the presence of C, O, S, Cl, among other traces of metallic elements.

No contribution for the N 1s (around 400 eV) was observed in the general survey and high resolution spectra between 395 and 408 eV. Then, the azo bond (–N=N–), aromatic amines and/or the dichlorotriazine groups were not detected. Considering these data, it is possible that the cleavage of the molecule occurred on the azo bond and/or the nitrogen linked to the naphthalene group. Consequently, the layer could be originated from disulphonate-naphthalene and/or hydroxy-sulphonate-naphthalene moieties. Deconvoluted high sensibility spectrum of the O 1s (Fig. 8b) revealed the presence of two bands at 531 and 531.9 eV corresponding to hydroxyl and sulphonate groups, respectively [69]. Carbon high sensibility spectrum (Fig. 8c) showed four deconvoluted bands at 284.6, 286.4, 289.4 and 290.9 eV. The band at 284.6 was attributed to C–C and C–H bonds, which are clearly present in naphthalene structure. Contribution at 286.4 eV is due to C–OH bond [70], present in the molecular structure of the hydroxy-naphthalene moiety. Signals at 289.4 and 290.9 eV are attributed to carbonate and polycarbonate groups [71], arisen from contamination. The S 2p analysis of high sensibility spectrum (Fig. 8d) revealed the presence of two bands at 168.5 and 169.8 eV (spin–orbit coupling), both attributed to sulphonate group [72,73].

Therefore, hydroxyl and sulphonate groups are present in the molecular structure of hydroxyl-sulphonate-naphthalene. According to this, this fragment could be responsible for the layer appeared on the cathode; but it cannot be discarded a mixed origin from the hydroxyl-sulphonate-naphthalene and disulphonate-naphthalene moieties combination.

4. Conclusions

The main conclusions of this work can be summarized in the following points:

- Spectroscopical studies indicated that both the electro-oxidation and electro-reduction treatments were able to degrade triazinic and azo groups. The electrochemical oxidation degraded the aromatic groups present in the dye molecule. Carbonyl groups were detected after the electrochemical oxidation of the dye and naphthalenic amines were formed during the azo group cleavage by electrochemical reduction of the dye solution.
- The decolourisation for all the electrolyses studied followed a pseudo-first order kinetic as HPLC measurements revealed. It was found that the current density influenced the rate constant of the electrochemical treatments. When electrochemical reduction was performed at 125 mA cm^{-2}, the process showed better results than at 250 mA cm^{-2}. In both cases, a brown layer appeared on the SS electrode surface.
- XPS and FTIR spectroscopy analyses of the layer revealed that it could be composed of two moieties of the dye molecule with similar structure: the hydroxyl-sulphonate-naphthalene and the disulphonate-naphthalene moieties.
- CV measurements showed the presence of adsorbed species on the electrode surface as a consequence of a degradation process

of the dye molecule during the electrochemical treatment. No spontaneous irreversible adsorption of the PMX2R molecule was found. In addition, a substantial dependence of the reduction process on the dye concentration was found.

Acknowledgements

The authors would like to acknowledge to the Spanish Ministry of Science and Innovation (MICINN) and European Union (FEDER funds) for the financial support (CTM2004-05774-C02-02 and CTM2007-66570-C02-02). A.I. del Río thanks to the Spanish Ministry of Science and Innovation (MICINN) her F.P.I. grant awarding. J. Molina is grateful to the Conselleria d'Empresa Universitat i Ciència (Generalitat Valenciana) for his FPI grant awarding.

References

[1] K.P. Sharma, S. Sharma, S. Sharma, P.K. Singh, S. Kumar, R. Grover, P.K. Sharma, A comparative study on characterization of textile wastewaters (untreated and treated) toxicity by chemical and biological test, Chemosphere 69 (2007) 48–54.
[2] S.M.A.G. Ulson de Souza, E. Forgiarini, A.A. Ulson de Souza, Toxicity of textile dyes and their degradation by the enzyme horseradish peroxidase (HRP), J. Hazard. Mater. 147 (2007) 1073–1078.
[3] C.A. Martínez-Huitle, E. Brillas, Decontamination of wastewaters containing synthetic organic dyes by electrochemical methods: a general review, 2008, doi:10.1016/j.apcatb.2008.09.017.
[4] C. Wang, A. Yediler, D. Lienert, Z. Wang, A. Kettrup, Ozonation of an azo dye C.I. Remazol Black 5 and toxicological assessment of its oxidation products, Chemosphere 52 (2003) 1225–1232.
[5] K. Swaminathan, S. Sandhya, S.A. Carmalin, K. Pachhade, Y.V. Subrahmanyam, Decolorization and degradation of H-acid and other dyes using ferrous–hydrogen peroxide system, Chemosphere 50 (2003) 619–625.
[6] M. Neamtu, A. Yediler, I. Siminiceanu, A. Kettrup, Oxidation of commercial reactive azo dye aqueous solutions by the photo-Fenton and Fenton-like processes, J. Photochem. Photobiol. A 161 (2003) 87–93.
[7] M.S. Lucas, A.A. Dias, A. Sampaio, C. Amaral, J.A. Peres, Degradation of a textile reactive azo dye by a combined chemical–biological process: Fenton's reagent-yeast, Water Res. 41 (2007) 1103–1109.
[8] L. Núñez, J.A. García-Hortal, F. Torrades, Study of kinetic parameters related to the decolourization and mineralization of reactive dyes from textile dyeing using Fenton and photo-Fenton processes, Dyes Pigments 75 (2007) 647–652.
[9] P. Peralta-Zamora, A. Kunz, S. Gomes de Moraes, R. Pelegrini, P. de Campos Moleiro, J. Reyes, N. Durán, Degradation of reactive dyes. I. A comparative study of ozonation, enzymatic and photochemical processes, Chemosphere 38 (1999) 835–852.
[10] M.M. Dávila-Jiménez, M.P. Elizalde-González, A.A. Peláez-Cid, Adsorption interaction between natural adsorbents and textile dyes in aqueous solution, Colloids Surf. A 254 (2005) 107–114.
[11] I. Sirés, N. Oturan, M.A. Oturan, R.M. Rodríguez, J.A. Garrido, E. Brillas, Electro-fenton degradation of antimicrobials triclosan and triclocarban, Electrochim. Acta 52 (2007) 5493–5503.
[12] I. Sirés, J.A. Garrido, R.M. Rodríguez, E. Brillas, N. Oturan, M.A. Oturan, Catalytic behaviour of the Fe^{3+}/Fe^{2+} system in the electro-Fenton degradation of the antimicrobial chlorophene, Appl. Catal. B 72 (2007) 382–394.
[13] A. Lahkimi, M.A. Oturan, N. Oturan, M. Chaouch, Removal of textile dyes from water by the electro-Fenton process, Environ. Chem. Lett. 5 (2007) 35–39.
[14] E. Guivarch, S. Trevin, C. Lahitte, M.A. Oturan, Degradation of azo dyes in water by electro-Fenton process, Environ. Chem. Lett. 1 (2003) 38–44.
[15] D. Genders, N. Weinberg, Electrochemistry for a Cleaner Environment, The Electrosynthesis Company Inc., New York, 1992.
[16] Y.M. Awad, N. Abuzaid, Electrochemical oxidation of phenol using graphite anodes, Sep. Sci. Technol. 34 (1999) 699–708.
[17] L. Fan, Y. Zhoub, W. Yang, G. Chen, F. Yang, Electrochemical degradation of Amaranth aqueous solution on ACF, J. Hazard. Mater. B 137 (2006) 1182–1188.
[18] M. Panizza, C. Bocca, G. Cerisola, Electrochemical treatment of wastewater containing polyaromatic organic pollutants, Water Res. 34 (2000) 2601–2605.
[19] F. Montilla, Fabricación y Caracterización de Nuevos Materiales Electródicos para la Transformación-Eliminación de Compuestos Aromáticos en Disolución Acuosa, Ph.D. thesis, Universidad de Alicante, Alicante, Spain, 2002.
[20] F. Montilla, E. Morallón, J.L. Vázquez, Electrochemical study of benzene on Pt of various surface structures in alkaline and acidic solutions, Electrochim. Acta 47 (2002) 4399–4406.
[21] L. Szpyrkowicza, S.N. Kaulb, R.N. Netib, S. Satyanarayanb, Influence of anode material on electrochemical oxidation for the treatment of tannery wastewater, Water Res. 39 (2005) 1601–1613.
[22] A. Perret, W. Haenni, N. Skinner, X.M. Tang, G. Gandini, Ch. Comninellis, B. Correa, G. Foti, Electrochemical behaviour of synthetic diamond thin film electrode, Diamond Relat. Mater. 8 (1999) 820–823.
[23] F. Montilla, P.A. Michaud, E. Morallón, J.L. Vázquez, Ch. Comninellis, Electrochemical oxidation of benzoic acid at boron-doped diamond electrodes, Electrochim. Acta 47 (2002) 3509–3513.
[24] X.M. Chen, G.H. Chen, F.R. Gao, P.L. Yue, High-performance Ti/BDD electrodes for pollutant oxidation, Environ. Sci. Technol. 37 (2003) 5021–5026.
[25] C. Saez, M. Panizza, M.A. Rodrigo, G. Cerisola, Electrochemical incineration of dyes using a boron-doped diamond anode, J. Chem. Technol. Biotechnol. 82 (2007) 575–581.
[26] F.H. Oliveira, M.E. Osugi, F.M.M. Paschoal, D. Profeti, P. Olivi, M.V.B. Zanoni, Electrochemical oxidation of an acid dye by active chlorine generated using $Ti/Sn_{(1-x)}Ir_xO_2$ electrodes, J. Appl. Electrochem. 37 (2007) 583–592.
[27] N. Mohan, N. Balasubramanian, C.A. Basha, Electrochemical oxidation of textile wastewater and its reuse, J. Hazard. Mater. 147 (2007) 644–651.
[28] G.R.P. Malpass, D.W. Miwa, S.A.S. Machado, A.J. Motheo, Decolourisation of real textile waste using electrochemical techniques: effect of electrode composition, J. Hazard. Mater. 156 (2008) 170–177.
[29] M. Gonçalves, M.M. Alves, J.P. Correia, I.P. Marques, Electrooxidation as the anaerobic pre-treatment of fats: oleate conversion using RuO_2 and IrO_2 based anodes, Bioresour. Technol. 99 (2008) 8207–8211.
[30] S. Stucki, R. Kotz, B. Carcer, W. Suter, Electrochemical wastewater treatment using high overvoltage anodes. II: anode performance and applications, J. Appl. Electrochem. 21 (1991) 99–104.
[31] J. Iniesta, P.A. Michaud, M. Panizza, G. Cerisola, A. Aldaz, Ch. Comninellis, Electrochemical oxidation of phenol at boron-doped diamond electrode, Electrochim. Acta 46 (2001) 3573–3578.
[32] J. Hastie, D. Bejan, M. Teutli-León, N.J. Bunce, Electrochemical methods for degradation of Orange II (sodium 4-(2-hydroxy-1-naphthylazo)benzenesulfonate), Ind. Eng. Chem. Res. 45 (2006) 4898–4904.
[33] Y.H. Wang, K.Y. Chan, X.Y. Li, S.K. So, Electrochemical degradation of 4-chlorophenol at nickel-antimony doped tin oxide electrode, Chemosphere 65 (2006) 1087–1093.
[34] S. Agarwal, P. Cluxton, M. Kemper, D.D. Dionysiou, S.R. Al-Abed, Assessment of the functionality of a pilot-scale reactor and its potential for electrochemical degradation of calmagite, a sulfonated azo-dye, Chemosphere 73 (2008) 837–843.
[35] M.C. Gutiérrez, M. Pepió, M. Crespi, Electrochemical oxidation of reactive dyes: method validation and application, Color. Technol. 118 (2002) 1–5.
[36] M. Panizza, G. Cerisola, Electrochemical oxidation as a final treatment of synthetic tannery wastewater, Environ. Sci. Technol. 38 (2004) 5470–5475.
[37] A. Fernandes, M. Morao, M. Magrinho, A. Lopes, I. Gonçalves, Electrochemical degradation of C.I. Acid Orange 7, Dyes Pigments 61 (2004) 287–296.
[38] A.S. Koparal, Y. Yavuz, C. Gürel, Ü.B. Ögütveren, Electrochemical degradation and toxicity reduction of C.I. Basic Red 29 solution and textile wastewater by using diamond anode, J. Hazard. Mater. 145 (2007) 100–108.
[39] M. Hamza, R. Abdelhedi, E. Brillas, I. Sirés, Comparative electrochemical degradation of the triphenylmethane dye methyl violet with boron-doped diamond and Pt anodes, J. Electroanal. Chem. 627 (2009) 41–50.
[40] L. Ciríaco, C. Anjo, J. Correia, M.J. Pacheco, A. Lopes, Electrochemical degradation of Ibuprofen on $Ti/Pt/PbO_2$ and Si/BDD electrodes, Electrochim. Acta 54 (2009) 1464–1472.
[41] M. Wu, G. Zhao, M. Li, L. Liu, D. Li, Applicability of boron-doped diamond electrode to the degradation of chloride-mediated and chloride-free wastewaters, J. Hazard. Mater. 163 (2009) 26–31.
[42] K. Muthukumar, P.S. Sundaram, N. Anantharaman, C.A. Basha, Treatment of textile dye wastewater by using an electrochemical bipolar disc stack reactor, J. Chem. Technol. Biotechnol. 79 (2004) 1135–1141.
[43] N. Mohan, N. Balasubramanian, In situ electrocatalytic oxidation of acid violet 12 dye effluent, J. Hazard. Mater. B 136 (2006) 239–243.
[44] D. Rajkumar, B. Joo Song, J. Guk Kim, Electrochemical degradation of Reactive Blue 19 in chloride medium for the treatment of textile dyeing wastewater with identification of intermediate compounds, Dyes Pigments 72 (2007) 1–7.
[45] A. Sakalis, D. Vanerková, M. Holcapek, P. Jandera, A. Voulgaropoulos, Electrochemical treatment of a simple azo dye and analysis of the degradation products using high performance liquid chromatography–diode array detection–tandem mass spectrometry, Chemosphere 67 (2007) 1940–1948.
[46] J. Bandara, P.T. Wansapura, S.P.B. Jayathilaka, Indium tin oxide coated conducting glass electrode for electrochemical destruction of textile colorants, Electrochim. Acta 52 (2007) 4161–4166.
[47] R. Jain, S. Varshney, S. Sikarwar, Electrochemical techniques for the removal of Reactofix Golden Yellow 3 RFN from industrial wastes, J. Colloid. Interface Sci. 313 (2007) 248–253.
[48] M. Muthukumar, M.T. Karuppiah, G.B. Raju, Electrochemical removal of C.I. Acid Orange 10 from aqueous solutions, Sep. Purif. Technol. 55 (2007) 198–205.
[49] E.-S.Z. El-Ashtoukhy, N.K. Amin, O. Abdelwahab, Treatment of paper mill effluents in a batch-stirred electrochemical tank reactor, Chem. Eng. J. 146 (2009) 205–210.
[50] K. Rajeshwar, J.G. Ibáñez, Environmental Electrochemistry: Fundamentals and Applications in Pollution Abatement, Academic Press, San Diego, 1997.
[51] M. Panizza, G. Cerisola, Removal of colour and COD from wastewater containing acid blue by electrochemical oxidation, J. Hazard. Mater. 153 (2007) 83–88.
[52] A.M. Faouzi, B. Nasr, G. Abdellatif, Electrochemical degradation of anthraquinone dye Alizarin Red S by anodic oxidation on boron-doped diamond, Dyes Pigments 73 (2007) 86–89.
[53] L. Fan, Y. Zhoub, W. Yang, G. Chen, F. Yang, Electrochemical degradation of aqueous solution of Amaranth azo dye on ACF under potentiostatic model, Dyes Pigments 76 (2008) 440–446.
[54] T. Bechtold, E. Burtscher, A. Turcanu, Cathodic decolourisation of textile waste water containing reactive dyes using a multi-cathode electrolyser, J. Chem. Technol. Biotechnol. 76 (2001) 303–311.

[55] T. Bechtold, A. Turcanu, Cathodic decolourisation of dyes in concentrates from nanofiltration and printing pastes, J. Appl. Electrochem. 34 (2004) 903–910.
[56] R.L.M. Allen, Colour Chemistry, Nelson & Sons, London, 1971.
[57] C. O'Neill, F.R. Hawkes, D.L. Hawkes, N.D. Lourenço, H.M. Pinheiro, W. Deleé, Colour in textile effluents—sources, measurement, discharge consents and simulation: a review, J. Chem. Technol. Biotechnol. 74 (1999) 1009–1018.
[58] J. Clavilier, The role of anion on the electrochemical behaviour of a {1 1 1} platinum surface; an unusual splitting of the voltammogram in the hydrogen region, J. Electroanal. Chem. 107 (1979) 211–216.
[59] F. Vicent, E. Morallón, C. Quijada, J.L. Vázquez, A. Aldaz, F. Cases, Characterization and stability of doped SnO_2 anodes, J. Appl. Electrochem. 28 (1998) 607–612.
[60] F. Montilla, E. Morallón, A. De Battisti, S. Barison, S. Daolio, J.L. Vázquez, Preparation and characterization of antimony-doped tin dioxide electrodes. Part 1. Electrochemical characterization, J. Phys. Chem. B 108 (2004) 5036–5043.
[61] F. Montilla, E. Morallón, A. De Battisti, A. Benedetti, H. Yamashita, J.L. Vázquez, Preparation and characterization of antimony-doped tin dioxide electrodes. Part 2. XRD and EXAFS characterization, J. Phys. Chem. B 108 (2004) 5044–5050.
[62] F. Montilla, E. Morallón, A. De Battisti, J.L. Vázquez, Preparation and characterization of antimony-doped tin dioxide electrodes. Part 3. XPS and SIMS characterization, J. Phys. Chem. B 108 (2004) 15976–15981.
[63] A.I. del Río, J. Molina, J. Bonastre, F. Cases, Influence of electrochemical reduction and oxidation processes on the decolourisation and degradation of C.I. Reactive Orange 4 solutions, Chemosphere (2009) 1329–1337.
[64] G. Sócrates, Infrared Characteristic Group Frequencies, John Wiley & Sons, Inc., 1997.
[65] L. Cohen, F. Soto, M.S. Luna, C.R. Praseti, G. Cassani, L. Faccetti, Analysis of sulfoxylated methyl esters (Φ-MES): sulfonic acid composition and isomer identification, J. Surfactants Deterg. (2006) 151–154.
[66] L. Xiao-Dong, L. Zi-sen, Determination of sulphonic compounds as their thiotrifluoroacetate derivatives by gas chromatography with ion trap detection, J. Chromatogr. A 667 (1994) 219–223.
[67] D. Pletcher, R. Greef, Instrumental Methods in Electrochemistry, Southampton Electrochemistry Group, Horwood, 2001.
[68] A. Bard, L.R. Faulkner, Electrochemical Methods, John Wiley & Sons, New York, 1980.
[69] C.D. Wagner, A.V. Naumkin, A. Kraut-Vass, J.W. Allison, C.J. Powell, J.R. Rumble Jr., X-ray Photoelectron Spectroscopy Database, The National Institute of Standards and Technology, U.S. Secretary of Commerce, 2002, http://www.srdata.nist.gov/xps.
[70] R. Benoit, C.N.R.S. Orléans, Y. Durand, B. Narjoux, G. Quintana, Y. Georges, X-ray Photoelectron Spectroscopy Database, La Surface, Thermo Electron Corporation, Thermo Electron France, http://www.lasurface.com/database/elementxps.php.
[71] M.M. Gorelova, V.Y. Levin, I.L. Dubchak, A.A. Zhdanov, L.I. Makarova, I.P. Storozhuk, S.S. Koroleva, An X-ray photoelectron spectroscopy study of the surface of siloxane-containing block copolymers, Polym. Sci. U.S.S.R. 31 (1989) 588.
[72] J.C. Lin, S.L. Cooper, Surface characterization and *ex vivo* blood compatibility study of plasma-modified small diameter tubing: effect of sulphur dioxide and hexamethyl-disiloxane plasmas, Biomaterials (1995) 1017–1023.
[73] R. Molina, J.P. Espinós, F. Yubero, P. Erra, A.R. González-Elipe, XPS analysis of down stream plasma treated wool: Influence of the nature of the gas on the surface modification of wool, Appl. Surf. Sci. (2005) 1417–1429.